Design and test of 704 MHz and 2.1 GHz normal conducting cavities for low energy RHIC electron cooler

Binping Xiao,* S. Belomestnykh,† J. M. Brennan, J. C. Brutus, G. McIntyre, K. Mernick, C. Pai, K. Smith, T. Xin, and A. Zaltsman
Brookhaven National Laboratory (BNL), Upton, New York 11973-5000, USA

V. Veshcherevich
Cornell University, Ithaca, New York 14853, USA

(Received 9 April 2018; published 5 March 2019)

The low energy RHIC electron cooler (LEReC) is currently under commissioning at BNL to improve RHIC luminosity for heavy ion beam energies below 10 GeV/nucleon. The linac of LEReC consists of a dc photoemission gun, one 704 MHz superconducting radio frequency booster cavity, and three normal conducting cavities. It is designed to deliver a 1.6–2.6 MeV electron beam, with peak-to-peak momentum spread dp/p of less than $\pm 7 \times 10^{-4}$. Two of the three normal conducting cavities will be used in LEReC for energy spread correction: a single-cell 704 MHz cavity for energy dechirping and a three-cell 2.1 GHz third harmonic cavity for rf curvature correction. In this paper, we present the designs and rf test results of these two cavities.

DOI: 10.1103/PhysRevAccelBeams.22.030101

I. INTRODUCTION

A bunched beam electron cooler called the low energy RHIC electron cooler (LEReC) [1] has been designed and constructed and is under commissioning at the Relativistic Heavy Ion Collider (RHIC) to significantly improve the collider luminosity at energies below 10 GeV/nucleon to map the QCD phase diagram, especially to search for the QCD critical point.

The ion beam in RHIC to be cooled consists of 111 bunches plus nine missing bunches for the abort gap, that are evenly distributed in the 3833.84 m circumference, with γ ranging from 4.1 to 6.1. It uses a 9 MHz rf system with a wide tuning range. In this paper, 9 MHz refers to the 120th harmonic of the RHIC revolution frequency, ranging from 9.104 to 9.256 MHz in LEReC. The ion bunches at $\gamma = 4.1$ are long (3 m rms length) in this case. The LEReC design is a nonmagnetized cooling approach that uses up to 30 flattop electron bunches spaced by 1.42 ns, with a <40% duty factor at kinetic energies between 1.6 and 2.6 MeV that match the ion beam velocity, to cool each single ion bunch. The detailed electron and ion beam structures are shown in Fig. 1. The pulsed modes of three discrete electron kinetic energies were proposed: 1.6, 2.0, and 2.6 MeV. A ± 0.1 MeV shift is allowed on these proposed energy levels. A mode of 1.6 MeV operation with a full continuous wave (cw) at the 704 MHz frequency (no macrobunches) is also being considered. Please note that there are electron bunches in the ion abort gap [2].

The electron linac of LEReC consists of a dc photoemission gun, one 704 MHz superconducting radio frequency (SRF) booster cavity [3], and three normal conducting cavities: a 2.1 GHz third harmonic cavity, a 704 MHz cavity [4], and a 9 MHz cavity. The 704 MHz SRF booster cavity accelerates 400 keV bunches from the dc gun near the top of the rf wave, with an accelerating voltage up to 2.2 MV. The booster also introduces an energy chirp for ballistic stretching of the bunches in the beam transport section. The remaining curvature of the bunch in longitudinal phase space is then corrected by decelerating the beam in the 2.1 GHz third harmonic cavity, so that the bunch is nearly linear in phase space. After the 30-m-long transport section, the bunch is still short enough so that the energy chirp can be removed with the normal conducting 704 MHz cavity [2].

The beam loading effect brought by the shunt impedance of the operating mode in each cavity was evaluated during the LEReC optical design, together with the curvature brought by the operating mode described above and the voltage fluctuation in the dc photoemission gun. The energy spread from these effects is suppressed using the low-level rf (LLRF) system of each cavity by carefully

*binping@bnl.gov
†Present address: Fermi National Accelerator Laboratory, Batavia, IL 60510-5011, USA.

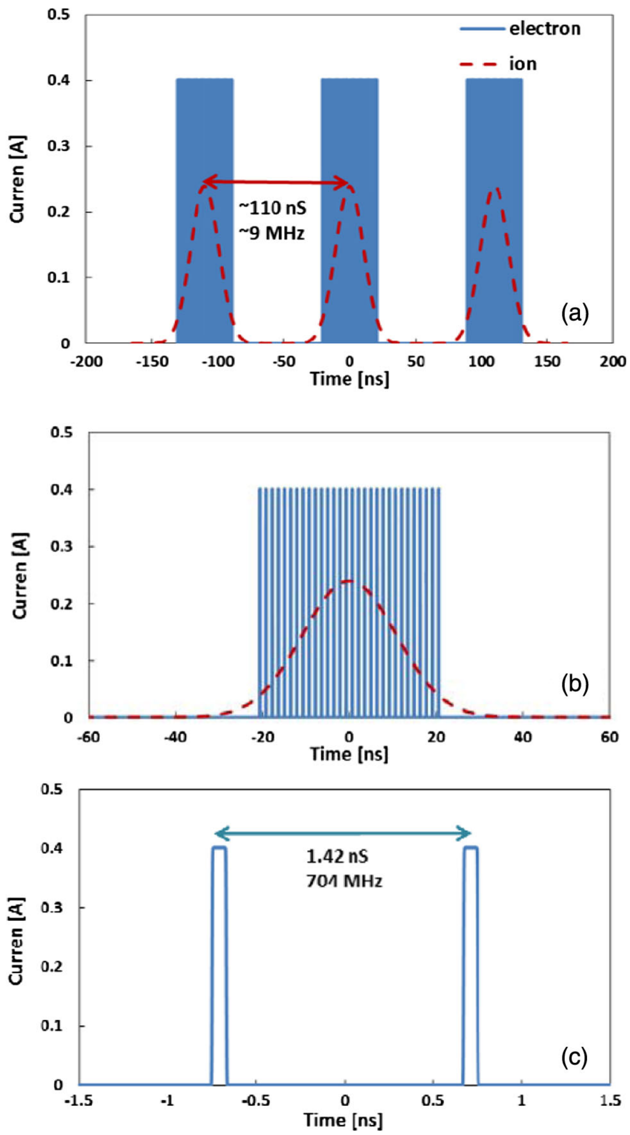

FIG. 1. Electron (blue solid line) and ion (red dashed line) beam pattern. (a) Three 9 MHz bunch trains; (b) one 9 MHz ion bunch with one electron bunch train that consists of 30 flattop electron bunches; (c) two adjacent flattop electron bunches that are spaced 1.42 nS, corresponding to 704 MHz.

choosing the working phase for the head-to-tail energy spread, together with a tunable 9 MHz ferrite cavity [5] to compensate the bunch-to-bunch energy spread within a macrobunch in pulsed modes. The systematic consideration of actively controlling the beam loading effect is not presented in this paper, which is dedicated to 2.1 GHz and 704 MHz normal conducting cavities.

The design of these two cavities is an iteration between cavity rf design and a multibunch wakefield-induced energy spread simulation; its workflow is (i) rf design of the cavities was performed to reach a reasonably high shunt impedance; (ii) higher-order modes (HOMs), as well as possible same-order modes (SOMs, $\pi/3$ and $2\pi/3$ TM_{010} modes that have the same order as the TM_{010} π mode in a three-cell cavity), were calculated; (iii) we then calculated the energy spread caused by the HOMs and SOMs in the worst case and found the dangerous mode(s); (iv) the results are fed back to step (i) to further optimize the cavity to suppress the dangerous HOMs. The decision was made that the impedance of dangerous mode(s) should first be suppressed by cavity shape optimization, as shown in step (iv). During this step, a small percentage reduction of the shunt impedance of the fundamental mode can be tolerated, since these cavities work in a reasonable voltage range. After this step, if there exist multiple dangerous modes in one cavity, a damper design should be employed. Since there is only one dangerous mode in each cavity after iterative optimization, as shown in Secs. II and III, instead of a damper, we choose to tune the 9 MHz frequency by carefully selecting the ion energy levels and/or to tune the frequency of this dangerous mode, to ensure the HOM-induced longitudinal momentum spread meets the specification.

The paper is organized as follows: first, the rf design of the cavities is introduced; then, the energy spread caused by HOMs and SOMs is considered and is fed back to the design of the cavities; after that, the frequency tuner and the fundamental power coupler (FPC) designs are presented; thermal and mechanical simulations are described in Sec. VI, followed by the rf test results, and the final cavity HOM and electron beam parameters in the last section before the conclusions section. The rf design optimization was performed using CST Microwave Studio® [6], and the final designs were simulated using ACE3P package [7]. The wakefield simulation was done using CST Particle Studio® [6]. Multipacting was simulated using the ACE3P package and then cross-checked with a GPU-based code [8]. Thermal and mechanical simulations were performed using ANSYS™ [9].

II. RF DESIGN OF THE CAVITIES

The 2.1 GHz cavity is a three-cell cavity operating at 2.112 GHz. It delivers an accelerating voltage up to 250 kV, at 9 kW power dissipation in the cavity walls with an unloaded quality factor Q of 20 000, and 21.2 kW maximum power from the beam (decelerating). The 704 MHz cavity is a single-cell structure operating at 704.0 MHz that delivers a voltage up to 251 kV, at 9.5 kW power dissipation in the cavity walls with an unloaded Q of 34 000, and 13.4 kW maximum power to the beam (accelerating). The parameters of these two cavities are listed in Table I. A 65 kW inductive output tube amplifier is chosen for the 704 MHz cavity, since it is readily available.

A. 2.1 GHz cavity

The cross-section view of the 2.1 GHz cavity is shown in Fig. 2. A pillbox-shape cell is adopted in this design. The wall between the adjacent cells is 10 mm thick, with the length of the vacuum portion of the center cell of

TABLE I. Parameters of the 2.1 GHz and 704 MHz normal conducting cavities.

Cavity	2.1 GHz	704 MHz
Frequency (MHz)	2112.0	704.0
Tuning range (MHz)	−1.2 to +2.9	−1.0 to +1.7
Number of cells	3	1
Voltage (kV)	250	251
R/Q (Ohm)	350	192
Q_0	20 000	34 000
FPC $Q_{\rm ext}$	20 000	14 000
Cavity power loss (kW)	9.0	9.5
Max beam power (kW)	−21.2	13.4
rf amplifier power (kW)	14	65

$(\lambda/2\text{–}10)$ mm, where λ is the wavelength. Cell-to-cell coupling is determined by a 47.6 mm diameter drift tube between the cells. Cells with different nose cone heights, shown in Fig. 2(i), were simulated to improve the cavity shunt impedance R_0 at $f_0 = 2.112$ GHz. For each simulation, the cavity radius is adjusted so that the TM_{010} π-mode resonance frequency is maintained at f_0. The simulations showed maximum R_0 at a 2.5 mm nose cone height. For the end cells, the nose cone close to the center

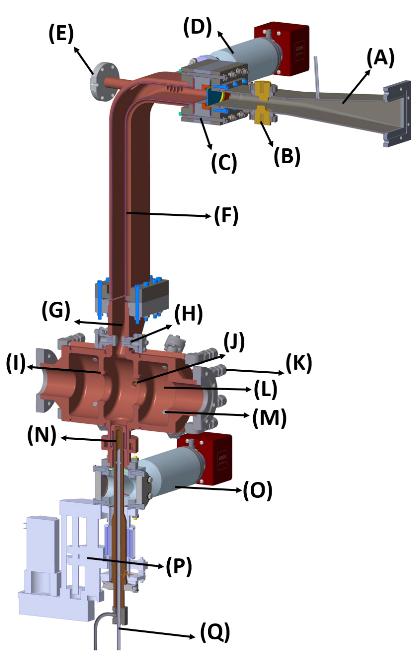

FIG. 2. A 2.1 GHz cavity cross section view. (a) Waveguide adaptor from JLab530 to WR430; (b) bolt with a nonconcentric knob; (c) JLab C100 rf window; (d) vacuum pump near the rf window; (e) view port; (f) FPC waveguide; (g) FPC port; (h) FPC tuner; (i) nose cone; (j) pickup coupler; (k) cavity water cooling channel; (l) cavity body; (m) fixed tuner; (n) main frequency tuner; (o) vacuum pump at the main tuner; (p) driver for the main tuner; (q) main tuner water cooling channel.

cell side is chosen to be the same as that for the center cell. No nose cone on the beam pipe side of the end cells is designed to simplify the cavity construction with 0.2% degradation of the shunt impedance on each end cell when compared with the end cell with the nose cone. The length of the end cell is chosen to be $(\lambda/2\text{–}10)$ mm, and the beam pipe on each end cell is 48.9 mm in diameter, to suppress the bunch-to-bunch (interbunch) energy spread, as shown in Sec. III A.

Two rf pickup ports, one shown in Fig. 2(j), are designed on the center cell of the cavity. A hook-shaped coupler is used to get 10 W rf power out of the cavity at 250 kV. This 10 W power will get significantly attenuated due to losses in an rf cable from the cavity location at the RHIC interaction region 2 (IR2) to the LLRF controller outside the RHIC tunnel. The output power can be adjusted by rotating the hook coupler.

With the 48.9 mm diameter beam pipe, it is easy to evacuate the cavity directly from the beam pipe. Thus, there is no pumping port on the cavity body.

An rf window [Fig. 2(b), with details shown in Fig. 7 (left)] with a transition taper to the WR430 waveguide is attached to the cavity via a 90°, 50.1 mm radius *E*-bend waveguide. A 15.9 mm blending radius is applied all around the rf coupling slot located on the center cell. A *V*-shaped FPC port is shown in Fig. 2(g), with an enlarged view in Fig. 7 (right). Details of the FPC design are described in Sec. V.

B. 704 MHz cavity

The 704 MHz normal conducting cavity serves not only as a dechirping cavity, but also as an accelerating cavity. Depending on the kinetic energy of the electron beam, the voltage and phase requirements change. The requirements are shown in Table II for four proposed operating modes.

A variety of shapes were considered: a pillbox shape, a toroidal shape previously designed for the Next Linear Collider (NLC) at Lawrence Berkeley National Laboratory (Berkeley Lab) [10], and an elliptical shape. The geometry chosen for the 704 MHz cavity is a variation of the toroidal shape. It is 213.1 mm long and has a 165.0 mm radius at the equator with rounded corners (rounding radius 86.1 mm) and an 82 mm beam pipe diameter, as shown in Fig. 3(g). It differs from the NLC shape [10] by the addition of a 40.9 mm straight section at the equator to ease fabrication of the FPC, tuner, vacuum pump, and rf pickup ports. The vacuum pump port, shown in Fig. 3(f), was designed 90° away azimuthally from the FPC port [Fig. 3(c)]. A metal mesh is installed on the port flange to block the rf field from penetrating toward the vacuum pump. Two rf pickup ports are located on the side opposite to the vacuum pump port. A hook-shaped coupler is used on each port to get a maximum of 2 W power out of the cavity at 250 kV.

TABLE II. Requirements of the 704 MHz cavity at different operating modes.

Operation mode	1.6 MeV	1.6 MeV cw	2.0 MeV	2.6 MeV
Bunch charge (pC)	130	120.8	170	200
Value of 9 MHz (MHz)	9.104	9.104	9.187	9.256
Bunches per macrobunch (9 MHz)	30	cw	30	24–30
Beam current (mA)	35.9	85.0	47.0	44.2–55.3
h of 704 MHz	9279	9279	9195	9127
Voltage (kV)	57.0	57.0	77.8	250.7
Phase (degree)	−78.9	−78.9	−76.2	−15.4
Acceleration (keV)	11.0	11.0	18.6	241.7
Power to beam (W)	394.1	933.2	871.5	13 354
Power on cavity (W)	492.3	492.3	917.1	9523
FPC coupling coefficient	1.80	2.90	1.95	2.40

III. HOM CONSIDERATION

As described in Ref. [3], 32 Gaussian laser pulses with 0.6 mm rms length are stacked together with a 0.75 mm interval to form a 24 mm "flattop" pulse. It is used to drive a dc photoemission gun [11] with a multialkali (CsK_2Sb or NaK_2Sb) cathode.

To calculate the bunch-to-bunch energy spread from the long-range wakefield of the longitudinal modes, a straightforward way is to "shift and stack" (based on the bunch pattern) the short-range wakefield of a single bunch, which can be simulated using CST Particle Studio™, to get the final result [3]. This method is not used because (i) it is time consuming (need to calculate the single-bunch wakefield until all modes are damped, and the shift and stack is also time consuming); (ii) one cannot apply the "worst case scenario," which is introduced in the next paragraph, by shifting the HOM frequency around, since the actual HOM frequency in the cavity might deviate from the rf simulation due to fabrication errors, thermal and mechanical deformations, frequency tuning of the fundamental mode, etc.; and (iii) one needs to evaluate the HOMs, find the dangerous ones, and modify the cavity rf design accordingly to suppress them.

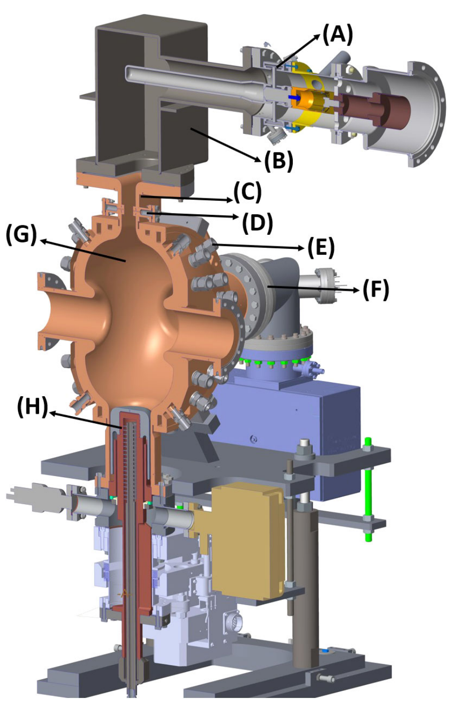

FIG. 3. A 704 MHz cavity cross section view. (a) Toshiba rf window; (b) WR1150 waveguide to coaxial transition piece; (c) FPC port; (d) FPC tuner; (e) cavity water cooling channel; (f) vacuum pump; (g) cavity body; (h) main frequency tuner.

We have employed a different method. First, an eigenmode simulation is done using CST Microwave Studio™, with the simulation frequency ranging from the fundamental mode to the first longitudinal cutoff, f_c, of the beam pipe. The wake impedances calculated from the single-bunch wake potential suggest that there is no high shunt impedance (trapped) mode beyond f_c and within the real bunch spectral range in these two cavities that will cause a significant energy spread. The eigenmode simulation results are then treated with a worst case scenario by artificially changing the resonance frequency of each HOM to a multiple of 9 MHz and for those modes that are close (± 20 MHz) to the multiples of 704 MHz. The single-bunch wake potential is then constructed using the "treated" eigenmode results with a bunch shape close to reality. The multibunch multitrain wake potential is calculated by using the shift and stack method on the single-bunch wake potential, with 30 continuous bunches (24–30 bunches for 2.6 MV operation) at the 704 MHz repetition frequency forming bunch trains at the 9 MHz repetition rate with an $\sim$40% duty factor and with continuous bunches with 704 MHz frequency for 1.6 MV cw operation.

In this paper, we use a rectangular (flattop) bunch instead of a delta function (point) bunch or Gaussian bunch calculated in Ref. [12], since it is closer to the real bunch shape generated by the laser pulses. For narrow band resonators with $Q \gg 1$, the wake potential of a flattop bunch that is normalized to one Coulomb bunch charge from each longitudinal mode can be calculated as

$$W_z(\tau) = \begin{cases} \frac{1}{T}\frac{R}{4Q^2} e^{-\frac{\omega\tau}{2Q}}[e^{\frac{\omega\tau}{2Q}} - \cos(\omega\tau) + 2Q\sin(\omega\tau)] & \text{for } 0 \le \tau \le T; \\ \frac{1}{T}\frac{R}{4Q^2} e^{-\frac{\omega\tau}{2Q}}\{e^{\frac{\omega T}{2Q}}\cos[\omega(T-\tau)] + 2Qe^{\frac{\omega T}{2Q}}\sin[\omega(T-\tau)] - \cos(\omega\tau) + 2Q\sin(\omega\tau)\} & \text{for } \tau > T. \end{cases}$$

In the above equations, ω, R, and Q are the angular resonance frequency, shunt impedance, and quality factor of a mode, respectively, and T is the bunch duration.

A. 2.1 GHz cavity

For the 2.1 GHz cavity, adjusting the end cell length might increase R_0. However, it will also increase the R/Q's of the SOMs, thus increasing the energy spread. For example, with the end cell lengthened by 10 mm, for the TM_{010} π mode, the R_0/Q will decrease by 2.7% and the Q will increase by 7.4%, which gives a 5% increase in R_0. However, alongside this change, the R/Q of the 2.099 GHz SOM increases from 0.07 Ω to 9.72 Ω. The frequency of this mode is mainly affected by the drift tube diameter between the cells, which determines the cell-to-cell coupling strength. It is not going to be a multiple of 704 MHz, since it is 13 MHz away from 2.112 GHz. However, it is possible for its frequency to be a multiple of 9 MHz, if the cell-to-cell coupling strength is altered, thus producing a high voltage fluctuation, estimated to be ∼5 kV, corresponding to the momentum spread of $\pm 2.5 \times 10^{-3}$, outside the required range. If the beam pipe diameter is set at 47.6 mm, the same as the diameter of the intercell drift tubes, the HOMs at 4.717 and 4.771 GHz will give a 0.73 kV voltage fluctuation, corresponding to $\pm 3.7 \times 10^{-4}$ dp/p. Setting the beam pipe diameter at 48.9 mm allows these HOMs to propagate out of the cavity, so that both R/Q's and Q's are suppressed. Therefore, we chose the length of the vacuum portion of the end cell to be $(\lambda/2 - 10)$ mm, and the beam pipe diameter to be 48.9 mm to reduce the SOM- or HOM-induced energy spread in this cavity [4]. With the 48.9 mm diameter beam pipe, the cutoff frequency is 3.60 GHz for the TE_{11} mode and 4.70 GHz for the TM_{01} mode.

After taking into account these considerations, there is only one mode, at 3.2808 GHz, that could drive the energy spread out of range if its frequency is at a multiple of 9 MHz. It is the TM_{011} $2\pi/3$ mode, with R/Q of 73.8 Ω and Q of 1.76×10^4. There are two SOMs associated with this mode, at 3.2574 GHz with R/Q of 10.5 Ω and at 3.3034 GHz with R/Q of 34.6 Ω. Both modes have Q factors about the same as the $2\pi/3$ mode and produce a <300 V fluctuation, which is still within the requirement. The field pattern of the 3.2808 GHz dangerous HOM is shown in Fig. 4. With this HOM, a bunch pattern with 28 bunches per train (while considering the 2.6 MeV operation with 24–30 bunches per 9 MHz macrobunch) gives a higher voltage fluctuation than that with 30 bunches per train. The reason is that its frequency is close to 4.66 times 704 MHz, the repetition rate of the bunches, so that the voltage fluctuation caused by this mode gets canceled every three bunches; thus, 30 bunches produce a relatively low voltage, and with 28 bunches, the last bunch produces a relatively large, ±1.82 kV, voltage fluctuation, corresponding to a $\pm 9.1 \times 10^{-4}$ dp/p for a 2 MeV beam. If we shift the 3.2808 GHz mode 0.5 MHz away from the harmonic of 9 MHz, it gives a voltage fluctuation of 0.67 kV, corresponding to $\pm 3.4 \times 10^{-4}$ dp/p. This 0.5 MHz difference can be reached by carefully choosing the ion beam energy and adjusting the electron energy to match the ion velocity, similar to Ref. [3], or using fixed tuners described in the next paragraph.

Eight fixed tuners, shown in Fig. 2(m), are evenly distributed along the equator of the end cells to provide enough frequency tuning range on the dangerous HOM and to minimize the transverse kick that might perturb the beam emittance, with four on each cell, 90° apart. These fixed tuners are used to tune the fundamental mode frequency towards 2.112 GHz (in combination with the frequency tuner shown in the next section) and to tune the 3.2808 GHz HOM [the main frequency tuner, shown in Fig. 2(n), will not affect this mode, because the field in the center cell is small] away from the multiples of 9 MHz. They are flush with the cavity inner surface in the nominal position. The simulation showed that, with one fixed tuner inserted 5 mm into the cavity, the TM_{010} π mode frequency increases by 0.36 MHz, and the frequency of the 3.2808 GHz HOM increases by 2.86 MHz. This tuning was done before evacuating the cavity. Jam nuts are used to ensure that the tuners stay in position during operation. During the bench test of the cavity with a network analyzer, two of the eight tuner ports were used as the coupling ports to measure

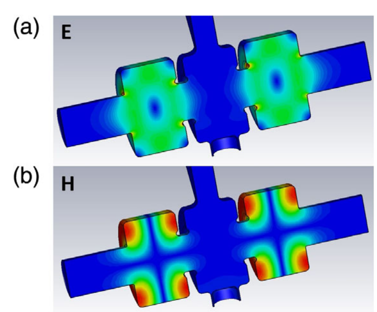

FIG. 4. Field pattern of the important 3.2808 GHz HOM in the 2.1 GHz warm cavity: (a) E field in the cross section; (b) H field in the cross section.

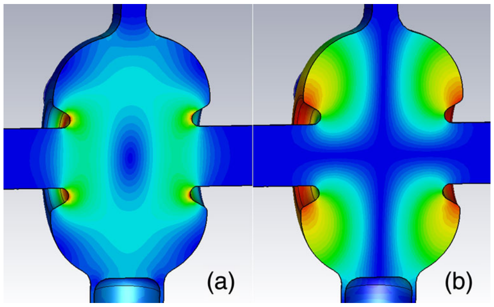

FIG. 5. Field pattern of the important 1.087 GHz HOM in the 704 MHz warm cavity: (a) E field in the cross section; (b) H field in the cross section.

some of the SOMs and HOMs (including the dangerous one) that have a low field in the center cell, where the FPC and pickup couplers located.

B. 704 MHz cavity

If the beam pipe diameter for the 2.1 GHz were used for the 704 MHz cavity, monopole HOMs at 1.087, 2.818, 3.523, and 4.227 GHz would have been trapped, and the HOM-induced bunch-to-bunch voltage fluctuation could be up to ~7.3 kV. By increasing the beam pipe to an 82 mm diameter, with the cutoff frequency of 2.14 GHz for the TE_{11} mode and 2.80 GHz for the TM_{01} mode, only the 1.087 GHz mode remains trapped. The drawback is that the fundamental mode R/Q degrades, increasing power dissipation in the cavity by ~25%, which is tolerable since the amplifier provides about 2 times more power than needed.

The voltage fluctuation is 2.11 kV with all HOMs in the worst case scenario. With the 1.087 GHz mode 1.0 MHz away from the harmonic of 9 MHz, the voltage fluctuation changes to 0.57 kV, corresponding to a $\pm 2.9 \times 10^{-4}$ dp/p for a 2 MeV beam.

The field pattern of the 1.087 GHz HOM is shown in Fig. 5. It is a TM_{011} mode. Unlike the 2.1 GHz cavity, in this cavity the dangerous HOM's frequency changes with the fundamental frequency tuner's location. It cannot be solely determined by fixed tuners. Using fixed tuners in this cavity is possible by carefully selecting locations for fixed tuners and then using a combination of a frequency tuner and fixed tuners to determine both the fundamental frequency and the dangerous HOM's frequency. It is not as straightforward as the 2.1 GHz cavity; thus, we choose not to have fixed tuners in the 704 MHz cavity.

IV. FREQUENCY TUNER DESIGN

The main frequency tuners are designed to be a folded coaxial structure, shown in Figs. 2(n) and 3(h), with an enlarged plot for the 2.1 GHz tuner in Fig. 6. The cavity fundamental mode couples to a TE_{11}-like mode in the coaxial line. This mode has a much higher cutoff frequency than that of the fundamental TM_{010} π mode, and it does not easily transform into the TEM mode. This design eliminates the rf contacts between moving parts in a traditional plunger-type tuner to improve reliability.

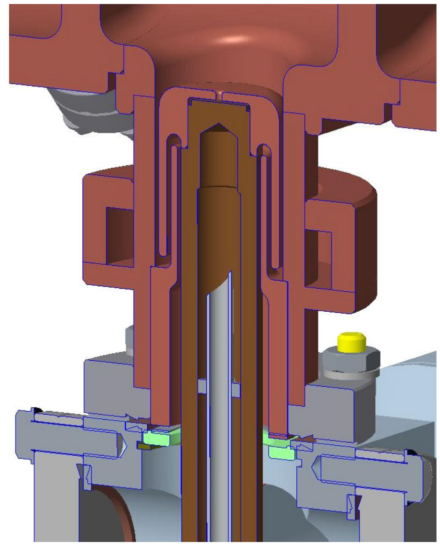

FIG. 6. Cross section of the folded coaxial tuner.

A. 2.1 GHz cavity

For simplicity, we used a straight (nonfolded) coaxial tuner model to estimate the length of the structure. The power leakage from the coaxial section is calculated by treating the end of the tuner as a waveguide port and calculating the power of the first five modes leaking out of the port. The results showed that a structure longer than 140 mm is needed to attenuate the power by −40 dB. Thus, in the case of a folded design, the tuner should be roughly 50 mm long. Additional length is needed to integrate bellows with the Lesker™ motor with part number 23HT18C230L500. It is important to note that a precise alignment of the tuner is necessary in this design. If the top of the tuner is shifted off axis or tilted by 0.1 mm, a factor of 40 times rf power is going to propagate out of the coaxial structure. For higher power application, especially in the cw mode, careful evaluation needs to be done, together with the thermal analysis of the tuner, which is described in Sec. VI.

This design was simulated for tuner penetrations from −6 to +6 mm, for which the fundamental frequency changes from −1.2 to +2.9 MHz with respect to the nominal. Simulations showed that multipacting barriers exist in this coaxial structure starting at 70 kV accelerating voltage. The tuner cap is designed to be demountable to provide the option of TiN coating for multipacting suppression [13].

B. 704 MHz cavity

The 704 MHz tuner is a 3∶1 scaled up version of the 2.1 GHz tuner. It is located opposite to the FPC port, shown in Fig. 3(h). With the tuner penetration varying from −12 to +12 mm, the frequency changes from −1.0 to +1.7 MHz with respect to the nominal frequency. From the simulation, multipacting is expected to start at 38 kV.

V. FPC DESIGN

A. 2.1 GHz cavity

For the 2.1 GHz cavity, the FPC is critically coupled to the cavity without a beam. In this case, there is no strong standing wave along the FPC waveguide, and the position of the FPC rf window is not critical with respect to the standing wave pattern. The rf window should not be in the line of sight of the electron beam to avoid charging of its ceramics, which may result in arcing through and creation of pinhole vacuum leaks [14].

Because of the time and budget limit, instead of designing a new rf window optimized for 2.1 GHz, a JLab C100/C50 rf window, shown in Fig. 2(c), with an enlarged view in Fig. 7 (left), was adopted for this cavity. It is placed after a 90° E bend of the 298-mm-long JLab530 rectangular waveguide with dimensions 134.4 mm by 25.0 mm, shown in Fig. 2(f). The TE_{10} cutoff frequency of the JLab530 waveguide is 1.134 GHz, and the TE_{20} cutoff frequency is 2.266 GHz. The cavity side of the rf window is under vacuum, with a pumping port and a view port close to the window [Figs. 2(d) and 2(e)]. The amplifier side is in air.

This rf window was originally designed for 1.5 GHz application at JLab; two knob tuners, shown in Fig. 2(b), with an enlarged view in Fig. 7 (left), are placed in the high electric field region of the air side to optimize the match at 2.112 GHz, which will cause some field enhancement. At 10 kW power delivered into the cavity, this should not cause a problem. The waveguide is then tapered to WR430 with dimensions 109.2 mm by 54.6 mm, shown in Fig. 2(a). The notch with less than −20 dB reflection at ∼2.1 GHz in S_{22} is sensitive to the position of the two knobs. With the knobs shifting by 0.2 mm along the waveguide, the notch frequency shifts by 26 MHz. The knob shifting is realized by rotating a bolt with an eccentric knob tip, shown in Fig. 7 (left). Multipacting simulations found no multipacting on the rf window in the accelerating voltage range from 1 to 250 kV with a 1.25 kV step size.

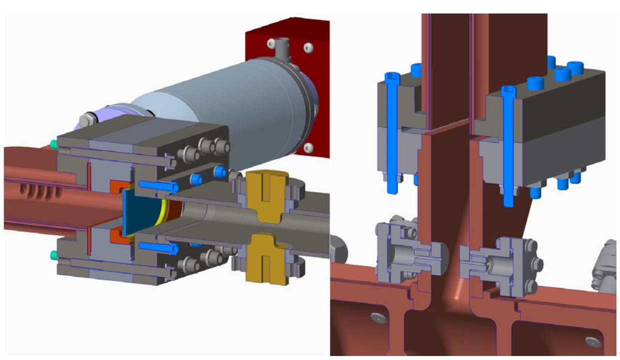

FIG. 7. Enlarged view of the JLab rf window with the pumping port and eccentric knobs (left, shown in yellow) and FPC coupling slot on the cavity with FPC tuners (right, shown in gray).

The FPC is designed to be critically coupled to the cavity with ideal Q. Surface roughness and brazing joints, as well as other imperfections, might give a degradation on the Q value, estimated to be up to 30%. Two FPC tuners, shown in Figs. 2(h) and 7 (right), are designed on the neck of the FPC port to adjust the coupling so that critical coupling can be met for different Q values. Two 12.7 mm diameter knobs with 5 mm insertion can adjust the Q_{ext} from 20 000 to 12 800.

The 2.1 GHz cavity operates at a beam phase near 180°, decelerating the beam. In this case, when the beam current increases, the cavity gets more power from the beam, thus needing less power from an rf amplifier. Figure 8 shows the calculation results of forward and reflected power at the FPC versus the beam current. The rf amplifier should provide 9 kW power to the cavity, and the reflected power will be less than 4 kW with a beam current up to 50 mA. Considering the waveguide loss, the amplifier should have an output power around 14 kW. The beam current, shown in Table II for both cavities, has four discrete levels: 35.9, 47.0, 55.3, and 85.0 mA. A maximum of 2.2 kW, and a minimum of 330 W, forward power is needed during the operation, corresponding to 35.9 and 85.0 mA, respectively. The 14-kW amplifier has good linearity at low power, so the cavity can be controlled by the rf system while the beam current is ramping up to 85.0 mA.

B. 704 MHz cavity

A Toshiba SNS-type coaxial window [15], shown in Fig. 3(a), is used on the 704 MHz cavity. The window is connected to the cavity using a WR1150 waveguide to coaxial line vacuum transition, as shown in Fig. 3(b). Multipacting simulations of this structure were performed from 10 to 500 kV accelerating voltage with a 10 kV step size, and no multipacting was found.

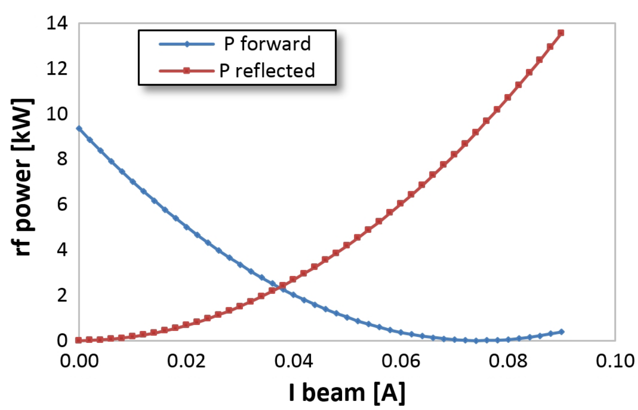

FIG. 8. A calculation of forward and reflected power at the 2.1 GHz cavity FPC versus the beam current at 250 kV cavity voltage.

To set the cavity critically coupled during operation with a beam, the FPC coupling coefficient would have to change from 1.8 to 2.9, listed in Table II. As the FPC is not adjustable, the coupling coefficient is set to 2.4, providing unity coupling at the highest required power level. Similar to the 2.1 GHz cavity, two FPC tuners, shown in Fig. 3(d), are designed so that this requirement can be met. In these two cavities, the FPC tuners are placed at a reasonably high magnetic field area so that thin disks can be used to provide enough adjustment in the coupling strength. During the design, special attention was paid to the rf losses on the FPC tuners to ensure they work well within the operating conditions of the cavities.

VI. THERMAL AND MECHANICAL SIMULATIONS

A 3D coupled rf-thermal-structural analysis of the cavities has been performed using ANSYS^{TM} Multiphysics finite element code to confirm the structural stability and to evaluate the frequency shift resulting from heating and structural expansion.

A. 2.1 GHz cavity

The 2.1 GHz cavity, with a 9.5 kW power dissipation at 250 kV accelerating voltage, is cooled using 26 °C water at a flow rate of 4 GPM per cooling channel. Cavity cooling channels are shown in Fig. 2(k). The maximum temperature is 69 °C on the nose cones, shown in Fig. 9 (left). The tuner is cooled with 26 °C water at a 3 GPM flow rate. The tuner cooling channel is shown in Fig. 2(q). The maximum temperature is 155 °C, as reported in Ref. [16] and shown in Fig. 9 (right), with a tuner fully inserted (6 mm) into the cavity. The tuner will outgas at this temperature, and it is going to settle at a reasonable vacuum level. We choose to bake the cavity with the tuner at 200 °C to minimize the outgassing. During operation, we expect the tuner to be near 0 mm insertion, and the maximum temperature on the tuner will be lower. At 250 kV, a mechanical simulation showed a maximum radial deformation of 0.04 mm and a maximum axial deformation of 0.13 mm, with a maximum thermal stress near the nose cones of 4.8×10^7 Pa. A frequency shift of −1.2 MHz is associated with these deformations. The design is further optimized to compensate this effect by fine-tuning the cavity diameter to shift the cavity resonance frequency up by 1.2 MHz at room temperature without high rf power.

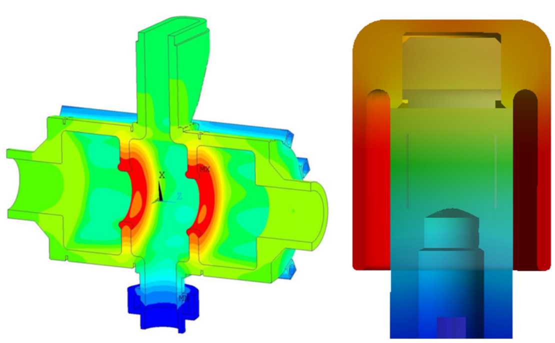

FIG. 9. Temperature distribution with 9 kW total power dissipation at 250 kV accelerating voltage (left) on the 2.1 GHz cavity wall with a maximum temperature at 69 °C and (right) on the tuner with a maximum temperature at 155 °C.

B. 704 MHz cavity

The 704 MHz cavity was originally designed for an accelerating voltage of 430 kV, resulting in 35.5 kW power dissipation in the cavity walls. In the final LEReC configuration, the maximum operating voltage will be only 250 kV with 9.5 kW wall dissipation power. The thermal and mechanical simulation were performed for the 430 kV case. The cavity is cooled using 32 °C water at a 20 GPM flow rate through cooling channels in the cavity walls as shown in Fig. 3(e). The maximum temperature is 64 °C at the blending radius of the FPC port. The mechanical simulation showed a maximum deformation of 0.14 mm and the corresponding von Mises stress of 3.4×10^7 Pa. Similar to the 2.1 GHz cavity, a frequency shift of −0.14 MHz is associated with these deformations and is compensated by fine-tuning the cavity diameter.

VII. RF TEST

A. 2.1 GHz cavity

With the main frequency tuner traveling from −6 to +6 mm, for the 2.1 GHz cavity without the FPC tuner, the FPC coupling coefficient was measured to be between 0.79 and 1.12 and the frequency between 2.1112 and 2.1153 GHz. The R/Q varies from 347.2 Ω to 350.7 Ω at the speed of light and the unloaded Q between 18 900 and 17 800. The reason for the FPC's external Q variation is due to the field flatness change: with the tuner inserted deeper into the cavity, the field is pushed to the end cells, which makes the coupling weaker and thus gives a higher Q_{ext}. Based on the measured Q value, the surface resistance showed 10% degradation from ideal polished copper.

With the copper main frequency tuner (without TiN coating), the cavity was high power conditioned to 240 kV in the cw mode and 250 kV in the 50% duty factor pulsed mode. The test was limited by thermal runaway of a power combiner and circulator of the rf power amplifier.

B. 704 MHz cavity

The 704 MHz cavity frequency was measured to be between 703.03 and 705.74 MHz and the unloaded Q between 33 700 and 31 000 with the main tuner traveling from −12 to +12 mm. Based on the Q value, the surface resistance showed 5% degradation from ideal polished copper. With two 6.4-mm-thick, 19.1 mm diameter tuners, the FPC coupling coefficient is measured to be 2.43.

TABLE III. Final HOM and electron beam parameters, and HOM-induced momentum spread in the worst case scenario, with the 2.1 GHz cavity dangerous HOM at 3282.17 MHz and the 704 MHz cavity dangerous HOM at 1084.54–1085.21 MHz. (The frequency of the dangerous HOM in this cavity changes with the main frequency tuner's position.)

Operation mode	1.60 MeV	1.60 MeV cw	1.92 MeV	2.60 MeV[a]
2.1 GHz cavity dangerous HOM away from 9 MHz (MHz)	4.55	Not applicable	2.09	3.75
dp/p from 2.1 GHz cavity HOMs [$\pm 10^{-4}$]	1.9	0.1	1.6	2.3
704 MHz cavity dangerous HOM away from 9 MHz (MHz)	>1.11	Not applicable	>2.02	>1.58
dp/p from 704 MHz cavity HOMs [$\pm 10^{-4}$]	3.6	0.1	3.0	2.2

[a]The dp/p for 2.60 MeV in this table is for the worst case in 24–30 bunch operation.

This cavity was high power conditioned to 250 kV in the cw mode. The cavity started to outgas at 37 kV, and at around 130 kV some multipacting activities appeared at the tuner port, accompanied by a pressure spike above the vacuum trip limit set at 5×10^{-6} Torr (6.7×10^{-4} Pa). This multipacting was conditioned away within half an hour.

VIII. FINAL HOM AND ELECTRON BEAM PARAMETERS

The dangerous HOM in the 2.1 GHz cavity is at 3282.17 MHz, with Q of 12 000 when all fixed tuners are flush with the cavity inner surface (the nominal position). It does not change with the main tuner location. With fixed tuners inserted into the cavity, the FPC coupling coefficient drops, the TM_{010} π-mode frequency increases by 0.38 MHz, and the dangerous HOM frequency drops by 2.1 MHz, for each fixed tuner with 5 mm insertion, close to the simulation results.

The dangerous HOM in the 704 MHz cavity is at 1084.94 MHz with the main tuner in its nominal position, with Q of 22 700. The design of the main tuner gives a large tuning range, from -12 to $+12$ mm, mainly to compensate the possible fundamental frequency deviation from the fabrication procedure. The fundamental frequency turned out to be 704.24 MHz with the main tuner at its nominal position. With the consideration of a maximum -0.14 MHz frequency shift due to the thermal deformation calculated above, during operation the tuning range will be within ± 0.3 MHz, corresponding to a ± 3 mm tuning range of the main tuner. Within this range, the dangerous HOM's frequency ranges from 1084.54 to 1085.21 MHz, with Q no more than 22 700.

The final selection of the HOM and electron beam parameters is shown in Table III. The fixed tuners in the 2.1 GHz cavity turned out to be at the nominal position with the consideration of the dangerous HOMs in these two normal conducting cavities and in the 704 MHz SRF booster cavity [3]. By carefully dealing with the dangerous HOM in each cavity, while the other HOMs are still considered to be in the worst case, the maximum longitudinal momentum spread is $\pm 5.5 \times 10^{-4}$, which meets the design requirement.

IX. CONCLUSIONS

Two normal conducting cavities with fundamental power couplers, rf windows, and frequency tuners were designed and built for the LEReC project. One cavity operates at the electron bunch repetition frequency of 704 MHz. The second cavity operates at the third harmonic. These cavities are used for beam energy spread correction. A combination of cavity shape optimization, frequency control of certain dangerous HOMs, and selection of operational energy levels was studied to suppress the SOMs and HOMs in these cavities so that the small energy spread specification can be met. A JLab C100/C50 rf window, which was originally designed for 1.5 GHz, was used on the 2.1 GHz cavity with two knob tuners for frequency matching. An SNS-type Toshiba window was used on the 704 MHz cavity. New coaxial tuners were designed to avoid rf fingers between moving components. Multiphysics simulations were performed to ensure the thermal and mechanical stability during operation. Both cavities were rf tested and high power conditioned up to 250 kV accelerating voltage to meet the operation requirements.

ACKNOWLEDGMENTS

The work is supported by Brookhaven National Lab (BNL) and/or Brookhaven Science Associates (BSA), LLC under Contract No. DE-AC02-98CH10886 with the U.S. DOE. This research used the resources of the National Energy Research Scientific Computing Center (NERSC), which is supported by the U.S. DOE under Contract No. DE-AC02-05CH11231. The authors thank M. Blaskiewicz, Wencan Xu, S. Polizzo, A. Fedotov, J. Tuozzolo, N. Laloudakis, and J. Butler for their help during the design and test of these two cavities.

[1] A. Fedotov *et al.*, Accelerator physics design requirements and challenges of RF based electron cooler LEReC, in *Proceedings of the North American Particle Accelerator Conference 2016, Chicago, IL, USA, 2016* (JACoW, Geneva, Switzerland, 2016)http://accelconf.web.cern.ch/AccelConf/napac2016/papers/wea4co05.pdf.

[2] J. Kewisch *et al.*, Beam optics for the RHIC Low Energy Electron Cooler (LEReC), in *Proceedings of the North American Particle Accelerator Conference 2016,*

Chicago, IL, USA (JACoW, Geneva, Switzerland, 2016), http://accelconf.web.cern.ch/AccelConf/napac2016/papers/wepob56.pdf.

[3] B. Xiao *et al.*, Higher order mode damper for low energy RHIC electron cooler superconducting radiofrequency booster cavity (to be published).

[4] B. P. Xiao *et al.*, HOM consideration of 704 MHz and 2.1 GHz cavities for LEReC linac, in *Proceedings of the 7th International Particle Accelerator Conference (IPAC'16), BEXCO, Busan, Korea* (JACoW, Geneva, Switzerland, 2016), http://accelconf.web.cern.ch/AccelConf/ipac2016/papers/mopmy009.pdf.

[5] S. Polizzo, 9 MHz LEReC cavity design, in *Proceedings of The Eighth Continuous Wave and High Average Power RF Workshop, Trieste, Italy, 2014*, https://indico.cern.ch/event/276274/contributions/625681/attachments/501434/692494/LeRHIC_9MHz_Cavity_Presentation_Slides.pdf.

[6] CST Studio Suite, http://www.cst.com/.

[7] ACE3P—Advanced Computational Electromagnetic Simulation Suite, https://confluence.slac.stanford.edu/display/AdvComp/Home.

[8] T. Xin *et al.*, A GPU based 3D particle tracking code for multipacting simulation, in *Proceedings of the 17th International Conference on RF Superconductivity (SRF2015), Whistler, BC, Canada* (United States Department of Energy, Office of Nuclear Physics, Washington, DC, 2015), http://srf2015.vrws.de/papers/mopb060.pdf.

[9] ANSYS, http://www.ansys.com.

[10] R. Rimmer *et al.*, RF Cavity R&D at LBNL for the NLC Damping Rings, CBP Technical Note No. 196 LCC-0033, 1999.

[11] K. Smolenski *et al.*, Design and performance of the Cornell ERL dc photoemission gun, Design and performance of the cornell ERL DC photoemission gun, AIP Conf. Proc. **1149** 1077 (2009).

[12] B. W. Zotter and S. A. Kheifets, *Impedances and Wakes in High-energy Particle Accelerators* (World Scientific, Singapore, 1998).

[13] P. He *et al.*, Secondary electron emission measurements for TiN coating on the stainless steel of SNS accumulator ring vacuum chamber, in *Proceedings of the 9th European Particle Accelerator Conference, Lucerne, 2004* (EPS-AG, Lucerne, 2004), http://accelconf.web.cern.ch/AccelConf/e04/PAPERS/WEPKF085.PDF.

[14] M. Drury *et al.*, Performance of the first refurbished CEBAF cryomodule, in *Proceedings of the 22nd Particle Accelerator Conference, PAC-2007, Albuquerque, NM* (IEEE, New York, 2007), p. 2478.

[15] I. Campisi *et al.*, The fundamental power coupler prototype for the spallation neutron source (sns) superconducting cavities, in *Proceedings of the 19th Particle Accelerator Conference, Chicago, IL, 2001* (IEEE, Piscataway, NJ, 2001), p. 1140.

[16] J. C. Brutus *et al.*, Mechanical design and 3-D coupled rf, thermal-structural analysis of normal conducting 704 MHz and 2.1 GHz cavities for LEReC linac, in *Proceedings of the 7th International Particle Accelerator Conference (IPAC'16), BEXCO, Busan, Korea, 2016* (JACoW, Geneva, Switzerland, 2016), MOPMY007, http://accelconf.web.cern.ch/AccelConf/ipac2016/papers/mopmy007.pdf.